Effect of valence electron concentration on the glass forming ability in Al-based alloys

É. Fazakas, L.K. Varga

***Abstract*— Metallic glasses-formation rules are mainly based on alloys with one or two principal components. The purpose of this paper is, by summarizing the microstructure characteristics of my and the reported Al-based glasses in terms of their atomic-size difference and enthalpy of mixing. The low GFA of Al- based alloys can be attributed to the relatively low heat of mixing and low relative atomic volume differences of the constituent elements. In addition, the lack of a deep eutectic at high Al-concentrations also contributes to the low GFA. By analyzing the density data of Al-based amorphous alloys, we have demonstrated that the atomic volumes (i.e., the metallic radii) are conserved during alloy formation and the rule of mixture can be applied for the average molar volume. A correlation was found between the crystallization temperatures and hardness values for the Al-based amorphous alloys. Furthermore, a correlation was found between the number of valence electrons and the hardness of Al-based amorphous alloys. In this way, an electronic rule for the formation of amorphous alloys with high thermal stability and strength could be established: the larger the average total electron number, e/a (or the Pauling valency, VEC), the better the strength and stability.**

***Index Terms*—GFA, VEC, Al-based amporphons.**

I. Results and Discussion

Although the theoretical and experimental investigations of GFA has made substantial advances in the last 20 years, not even at the present days can it be regarded a closed chapter in the materials physics. Many criteria of GFA have been forwarded even in the recent literature; however neither the range of validity, nor the connection between them seems to be clearly established. In practice of metallurgy the empirical rules of Inoue can be used only:

i) the averaged atomic size difference expressed by the Egami's λ parameter [1] should be higher than 0.1; ii) the heat of mixing should be negative and iii) the GFA, in general, is increasing with the number elements satisfying the former two conditions. The most popular compositions are ternary $Al_{100-x-y}LTM_xRE_y$ alloys ($5<x<10$, $2<y<10$), where LTM stands for late transition elements Ni, Co, Fe or a combination of them and RE stands for Y and rare earth elements or mischmetal.

Glass-forming ability involves two aspects: the stability of the liquid structure and the resistance to crystallization. The former is related to the thermodynamic factors, and the latter to the kinetic factors. Owing to the difficulties in measuring thermodynamic parameters directly from the liquid state, most indicators of GFA involve parameters measured or calculated from the solid state.

It is our conjecture, that one single indicator cannot be used to predict GFA. Therefore, the combination of multiple indicators may be a way more effective to evaluate GFA.

For a restricted family of amorphous alloys, like the Al–based amorphous alloys having Al content above 80 at%, the GFA tendency can be measured by the stability against the crystallization as it is expressed by the thermodynamically criteria. The thermal stability and the mechanical strength are both determined by the bond strength which in metallic alloys are strongly dependent on the electron per atom, e/a, number in the given alloy. This is why a correlation is expected between the microhardness and crystallization temperatures for Al-based amorphous alloys covering wide composition range. In this way the GFA can be measured by the value of the microhardness as well. In the following we combine our data with the literature data and the observed correlation will be used for designing new high temperature Al-based amorphous alloys.

Any calculations in this paper have been made on more than 30 own compositions and on some of the most representative amorphous compositions found in the literature.

II. Criteria Based on Atomic Size Mismatch

It is expected that GFA increases with increasing the overall atomic size mismatch.

Based on the atomic scale elasticity theory, Egami and Waseda [1] have suggested the following minimum solute content:

$$\chi_B^{\min}\left|\frac{V_B - V_A}{V_A}\right| = \chi_B^{\min}\left|\left(\frac{r_B}{r_A}\right)^3 - 1\right| \approx 0{,}1 \qquad (1)$$

where r_A and r_B are the solvent and solute atomic radius, respectively. V_A and V_B are the corresponding atomic volumes.

It turns out, that the larger the atomic size difference is, the smaller the amount of solute is required to form an amorphous phase. In the Table 1. the most important TM solute are collected:

É. Fazakas, Bay Zoltán Nonprofit Ltd. For Applied Research H-1116 Budapest, Fehérvári út 130, Hungary
L.K. Varga, Wigner Research Center for Physics, Hungarian Academy of Sciences, H-1525, P.O.B. 49, Hungary

Table 1. The minimum solute content for a glass forming Al-TM alloy

Element	Sc		Ti	V	Cr	Mn	Fe	Co	Ni	Cu	Zn
x_B^{min}(at%)	20		20	45	30	62	29	30	29	35	35
	Sr	**Y**	**Zr**	**Nb**	**Mo**					**Ag**	
	4	10	25	25	73					73	

The atomic size mismatch is usually expressed by the λ parameter of Egami and Waseda [1]: for a binary alloys:

$$\lambda = C_B\left|1-\left(\frac{R_B}{R_A}\right)^3\right| + C_C\left|1-\left(\frac{R_C}{R_A}\right)^3\right| \qquad (2)$$

and for a multicomponent alloy:

$$\lambda = \sum_{i=B}^{Z} C^i \cdot \left|\frac{r_i^3}{r_A^3}-1\right| = C^B \cdot \left|\frac{r_B^3}{r_A^3}-1\right| + \ldots + C^Z \cdot \left|\frac{r_Z^3}{r_A^3}-1\right| \qquad (3)$$

where A denotes the solvent element. According to the Egami and Waseda criterion the $\lambda > 0.1$ inequality should be satisfied for good GFA. In the case of Al–based amorphous alloys, however, amorphous alloys could be obtained even for $\lambda < 0.1$. Nevertheless, this criterion is useful also for the Al-based alloys as well, it predicts the existence of the prepeak in the DSC diagram corresponding to the precipitation of nano-Al phase for $\lambda < 0.1$ (amorphous behaviour) and the very probably endothermic peak (glass transition) before the main crystallization peak for $\lambda > 0.1$ (glassy behaviour).

Beside the expression of Egami and Waseda [1], there are other formulas to express the atomic mismatch. For example, the simple mean-square-root deviation of the atomic radii δ, introduced by Fang, et al [2]:

$$\delta = \sqrt{\sum_{i=1}^{n} C_i\left(1-\frac{r_i}{\bar{r}}\right)^2}, \bar{r} = \sum_{i=1}^{n} C_i r_i \qquad (4)$$

The coordination number of the solute atom depends on the Al-X bond distance. Trial and error experiments have shown that for good GFA, a structure of large (Y like) clusters or a combination of small (Co-like) and large (Y-like) clusters is preferred.

Senkov and Miracle [3] presented the atomic mismatch in a diagram showing the concentration of the element as a function of the atomic radii. He found the following correlation: concave curve for good glass formers and convex one for poor glass formers. Unfortunately, the Al-RE-TM-type amorphous alloys studied so far belong to the convex curve.

III. Criteria based on thermodynamic calculations

The negative heat of mixing can be estimated by the electronegativity difference between the constituents. In the case of a quaternary alloy series, such as Al_{85}(Y, Gd, Dy, Er, Sm, La, Ce)$_8Ni_5Co_2$, it was found experimentaly that the GFA expressed as the width of the supercooled liquid range T_x-T_g scales with the electronegativity difference between Al and RE element. However, this tendency to increase ΔT_x with electronegativity of solute is not followed for $Al_{85}Sc_8Ni_5Co_2$, although the electronegativity of Sc is 1.32 but λ=0.064. [4]. It seems that for good GFA, both the electronegativity and atomic size differences should be large.

More exact thermodynamic estimations can be made using the Miedema model for the calculation of the heat of mixing. The mixing enthalpy (ΔH) can be calculated based on the extended Miedema model for solid solutions as:

$$\Delta H = \sum_{\substack{i=1 \\ i\neq j}}^{3} \Omega_{ij} c_i c_j \qquad (5)$$

where Ω_{ij} is the regular solution interaction parameter between i-th and j-th elements and is equal to 4 times the heat of mixing: $\Omega_{ij} = \Delta H_{AB}^{mix}$ and c_i is the concentration of the i-th elements. The heats of mixing values are collected in the Tables 2/a, b and c [5] for the most important compositions for the present work.

Table 2/a Values of ΔH_{AB}^{mix} (kJ/mol) calculated by Miedema's model for atomic pairs between elements with Al-3d, Al-4d and Al-5d [Boer 1988].

	Al	Ca	Sc	Ti	V	Cr	Mn	Fe	Co	Ni	Cu	Zn
Al	0	-20	-38	-30	-16	-10	-19	-11	-19	-22	-1	1
Ca	-20	0	17	43	44	38	19	25	2	-7	-13	-22
Sc	-38	17	0	8	7	1	-8	-11	-30	-39	-24	-29
Ti	-30	43	8	0	-2	-7	-8	-17	-28	-35	-9	-15
V	-16	44	7	-2	0	-2	-1	7	14	-18	5	-2
Cr	-10	38	1	-7	-2	0	2	-1	-4	-7	12	5
Mn	-19	19	-8	-8	-1	2	0	0	-5	-8	4	-6
Fe	-11	25	-11	-17	7	-1	0	0	-1	-2	4	-6
Co	-19	2	-30	-28	14	-4	-5	-1	0	0	6	-5
Ni	-22	-7	-39	-35	-18	-7	-8	-2	0	0	4	-9
Cu	-1	-13	-24	-9	5	12	4	4	6	4	0	1

Zn	1	-22	-29	-15	-2	5	-6	-6	-5	-9	1	0	

Table 2/b and 2/c. Values of ΔH_{AB}^{mix} (kJ/mol) [Boer 1988].

	Al	**Y**	**Zr**	**Nb**	**Mo**
Al	0	-38	-44	-18	-5
Y	-38	0	9	30	24
Zr	-44	9	0	4	-6
Nb	-18	30	4	0	-6
Mo	-5	24	-6	-6	0

	Al	**La**	**Ce**	**Hf**	**Ta**	**W**	**U**
Al	0	-38	-38	-39	-19	-2	-30
La	-38	0	0	15	33	32	15
Ce	-38	0	0	14	31	29	14
Hf	-39	15	14	0	3	-6	-2
Ta	-19	33	31	3	0	-7	3
W	-2	32	29	-6	-7	0	1
U	-30	15	14	-2	3	1	0

Particularly, for the quasi-binary (Zr, Ti, Hf)-(Cu, Ni) systems, Basu et al [6] have found that the mixing enthalpy varies between -13 and -45 kJ/mol and the normalized mismatch entropy varies between 0.13 and 0.15.
For our Al-based amorphous alloys, similar diagram is shown in Fig.1. where the mixing enthalpy ranges between -8 kJ/mol and -16 kJ/mol and the normalized mismatch entropy varies between -13 kJ/mol and -42 kJ/mol.

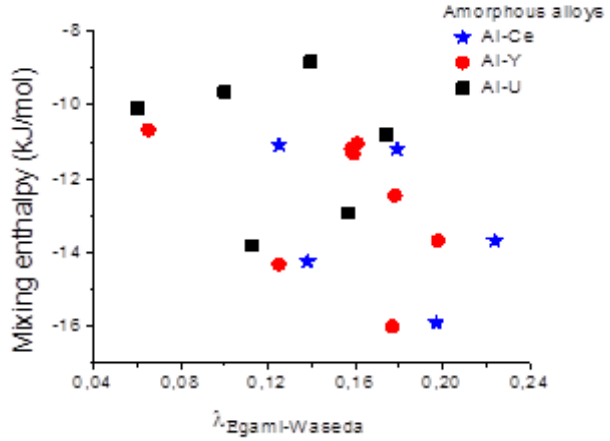

Figure 1. Mixing enthalpy as a function of λ parameter for our Al-based amorphous alloys (see Table 3.).

Table 3. List of the most representative Al-based metallic glasses published in the literature.

Al-based Metallic Glasses			
Binary	Ternary	Quaternary	Quintenary
$Al_{93}Ba_7$ [14]	$Al_{90}Ce_5Fe_5$ [20]	$Al_{85}Nd_8Ni_5Co_2$ [22]	$Al_{85}Y_4Nb_4Ni_5Co_2$ [14]
$Al_{93}Ca_7$ [14]	$Al_{90}Ce_7Co_3$ [14]	$Al_{88}Gd_6Er_2Ni_4$ [14]	$Al_{85}Y_6Ni_5Co_2Zr_2$ [14]
$Al_{92}Sm_8$ [16]	$Al_{86}La_5Ni_9$ [21]	$Al_{88}Ce_2Ni_9Fe_1$ [14]	$Al_{84}Y_6Ni_4Co_2Sc_4$ [14]
$Al_{92}La_8$ [17]	$Al_{88}Y_7Fe_5$ [14]	$Al_{88}Nd_5Ni_6Fe_1$ [22]	$Al_{85}Ni_5Y_6Co_2Fe_2$ [24]
$Al_{92}Ce_8$ [17]	$Al_{90}Nd_5Ni_5$ [14]	$Al_{87}Nd_3Ni_7Cu_3$ [22]	$Al_{85}Ni_4Y_6Co_3Fe_2$ [14]
$Al_{91}Y_9$ [17]	$Al_{88}Y_8Ni_4$ [14]	$Al_{85}Ce_5Ni_8Co_2$ [14]	$Al_{85}Ni_3Y_8Co_2Fe_2$ [14]
$Al_{90}La_{10}$ [18]	$Al_{90}Nd_5Fe_5$[22]	$Al_{83.5}Y_5Ni_{8.5}(Co,Fe)_3$[14]	$Al_{85}Ni_3Y_6Co_3Fe_3$ [14]
$Al_{68}Ge_{32}$ [14]	$Al_{89}Fe_{10}Zr_1$ [13]	$Al_{85}Y_8Ni_5Co_2$ [14]	$Al_{84}Ni_8Co_4Y_3Zr_1$ [28]
$Al_{90}Y_{10}$ [19]	$Al_{89}La_6Ni_5$ [14]	$Al_{84}Y_9Ni_5Co_2$ [27]	
	$Al_{87}Ce_3Ni_{10}$ [14]	$Al_{84.5}Y_8Ni_5Co_{2.5}$ [14]	
	$Al_{85}Ce_5Mg_{10}$ [14]	$Al_{84.5}Y_{8.5}Ni_5Co_2$ [14]	
	$Al_{85}Y_{10}Ni_5$ [23]		
	$Al_{75}Y_4Ni_{21}$ [24]		
	$Al_{84}Ni_{12}Zr_4$ [25]		
	$Al_{85}Y_{10}Ni_5$ [14]		
	$Al_{70}Si_{17}Fe_{13}$ [26]		

Table 4. Heat of mixing and atomic mismatch parameters for the Al-based amorphous. Data with novel elements, first published in the literature, are in italic.

Composition	**XRD**	**λ**	**δ**	**ΔH (kJ/mol)**
Binaries				
$Al_{92}Y_8$	AM	0,08	6,87	-11,187
$Al_{90}Y_{10}$	AM	0,1	7,56	-13,68
$Al_{88}Y_{12}$	AM+IM	0,12	8,16	-16,05
$Al_{92}Ce_8$	AM	0,09	7,9	-11,19
$Al_{90}Ce_{10}$	AM	0,12	7,92	13,68
$Al_{92}U_8$	*AM*	*0,06*	*2.45*	*8,832*
$Al_{90}U_{10}$	*AM*	*0,08*	*2,7*	*-10,8*
$Al_{90}Pd_{10}$	AM+IM	0,01	1,26	-16,56
$Al_{95.5}Cr_{14.5}$	AM+IM	0,041	3,75	-4,959
Composition	**XRD**	**λ**	**δ**	**ΔH (kJ/mol)**
$Al_{90}Mo_{10}$	AM+IM	0,0089	0,842	-3,65
$Al_{90}W_{10}$	AM+IM	0,0074	0,842	-0,72
$Al_{90}V_{10}$	AM+IM	0,018	1,9	-5,76
$Al_{90}Nb_{10}$	AM+IM	0,0056	6,28	-6,48
$Al_{90}Zr_{10}$	AM+IM	0,04	3,525	-15,84
Ternaries at the edge of GFA				
$Al_{92}Ni_4Ce_4$	AM	0.05	5.9	-9,01
$Al_{90}Ni_4Ce_6$	AM+IM	0.07	6,9	-11,65
$Al_{90}Ni_5Y_5$	AM+IM	0,03	6,4	-11.11
$Al_{90}Ni_5Ce_5$	AM+IM	0,04	6,6	-11.08
$Al_{90}Ni_5U_5$	*IM*	*0,03*	*3,6*	*-9,65*
$Al_{90}Ni_5Ti_5$	IM	0,016	3	-9,71
$Al_{90}Ni_5Zr_5$	IM	0,035	4	-12,37
$Al_{90}Ni_5Hf_5$	AM+IM	0,03	3,79	-11,4
$Al_{90}Ni_5V_5$	AM+IM	0,02	3,11	-7,02
$Al_{90}Ni_5Nb_5$	*IM*	*0,04*	*3*	*-7,5*
$Al_{90}Ni_5Ta_5$	*IM*	*0,035*	*2,95*	*-7,67*
$Al_{88}Ni_{10}Cu_2$	IM	0,036	4,25	-77,824
$Al_{88}Ni_{10}Co_2$	IM	0,036	4,35	-90,816
$Al_{88}Ni_{10}Fe_2$	IM	0,036	4,31	-85,344
$Al_{88}Ni_{10}Mn_2$	IM	0,036	4,31	-91,456
$Al_{88}Ni_{10}Cr_2$	IM	0,036	4,25	-8,504
$Al_{88}Ni_{10}V_2$	IM	0,034	4,08	-90,144
$Al_{88}Ni_{10}Ti_2$	AM+IM	0,032	4,06	-10,136
$Al_{88}Ni_{10}Y_2$	AM+IM	0,05	5,55	-1,06,672
$Al_{88}Ni_{10}U_2$	*AM*	*0,03*	*4,29*	*-10,088*
$Al_{89}Mg_3Mm_8$	*AM*	*0,084*	*7,35*	*-2,572*
$Al_{87}Mg_5Mm_8$	*AM +IM*	*0,0869*	*7,43*	*-29,048*
$Al_{87}Mg_7Mm_6$	*AM+IM*	*0,0702*	*6,76*	*-25,872*

$Al_{85}Nb_6Ni_9$	*AM*	*0,0151*	*0,04*	*-11,052*
$Al_{85}Ta_6Ni_9$	*AM*	*0,0151*	*0,04*	*-11,234*
Multicomponent Al-LTM				
$Al_{88}Co_4Ni_4Cu_4$	IM	0,03	4,02	-5,85
$Al_{85}Co_5Ni_5Cu_5$	IM	0,05	4,43	-7,04
$Al_{85}Cr_3Mn_3Fe_3Co_3Ni_3$	IM	0,05	4,3	-8,42
$Al_{85}Cr_{2.5}Mn_{2.5}Fe_{2.5}Co_{2.5}Ni_{2.5}Cu_{2.5}$	IM	0,048	4,2	-6,94
Quaternaries with RE				
Al90Ni8Ce1Fe1	AM+IM	0,02	4,7	-8,19
Al85Ce5Ni8Co2	AM	0,017	7,35	-4,236
Al85Y5Ni8Co2	AM	0,016	7,1	-14,32
Al85U5Ni8Co2	*AM*	*0,049*	*4,5*	*-12,932*
Al85Ce8Ni5Co2	AM	0,058	8,22	-15,90
Composition	**XRD**	**λ**	**δ**	**ΔH (kJ/mol)**
Al85Y8Ni5Co2	AM	0,056	7,9	-16,005
Al85U8Ni5Co2	*AM*	*0,048*	*4.3*	*-1,38,032*
Al88Y7Fe5	AM	0.085	7,15	-1,13,132
Al88Y7Fe4Sb1	*AM*	*0,073*	*7,08*	*-1,10,272*
Al-Si based				
Al79Si10Ni9Ti2	*AM*	*0,09*	*7.85*	*-16,377*
Composition	**XRD**	**λ**	**δ**	**ΔH (kJ/mol)**
Binaries				
$Al_{92}Y_8$	AM	0,08	6,87	-11,187
$Al_{90}Y_{10}$	AM	0,1	7,56	-13,68
$Al_{88}Y_{12}$	AM+IM	0,12	8,16	-16,05
$Al_{92}Ce_8$	AM	0,09	7,9	-11,19
$Al_{90}Ce_{10}$	AM	0,12	7,92	13,68
$Al_{92}U_8$	*AM*	*0,06*	*2.45*	*8,832*
$Al_{90}U_{10}$	*AM*	*0,08*	*2,7*	*-10,8*
$Al_{90}Pd_{10}$	AM+IM	0,01	1,26	-16,56
$Al_{95.5}Cr_{14.5}$	AM+IM	0,041	3,75	-4,959
Composition	**XRD**	**λ**	**δ**	**ΔH (kJ/mol)**
$Al_{90}Mo_{10}$	AM+IM	0,0089	0,842	-3,65
$Al_{90}W_{10}$	AM+IM	0,0074	0,842	-0,72
$Al_{90}V_{10}$	AM+IM	0,018	1,9	-5,76
$Al_{90}Nb_{10}$	AM+IM	0,0056	6,28	-6,48
$Al_{90}Zr_{10}$	AM+IM	0,04	3,525	-15,84
Ternaries at the edge of GFA				
$Al_{92}Ni_4Ce_4$	AM	0.05	5.9	-9,01
$Al_{90}Ni_4Ce_6$	AM+IM	0.07	6,9	-11,65
$Al_{90}Ni_5Y_5$	AM+IM	0,03	6,4	-11.11
$Al_{90}Ni_5Ce_5$	AM+IM	0,04	6,6	-11.08
$Al_{90}Ni_5U_5$	*IM*	*0,03*	*3,6*	*-9,65*
$Al_{90}Ni_5Ti_5$	IM	0,016	3	-9,71
$Al_{90}Ni_5Zr_5$	IM	0,035	4	-12,37
$Al_{90}Ni_5Hf_5$	AM+IM	0,03	3,79	-11,4
$Al_{90}Ni_5V_5$	AM+IM	0,02	3,11	-7,02
$Al_{90}Ni_5Nb_5$	*IM*	*0,04*	*3*	*-7,5*
$Al_{90}Ni_5Ta_5$	*IM*	*0,035*	*2,95*	*-7,67*
$Al_{88}Ni_{10}Cu_2$	IM	0,036	4,25	-77,824
$Al_{88}Ni_{10}Co_2$	IM	0,036	4,35	-90,816
$Al_{88}Ni_{10}Fe_2$	IM	0,036	4,31	-85,344
$Al_{88}Ni_{10}Mn_2$	IM	0,036	4,31	-91,456
$Al_{88}Ni_{10}Cr_2$	IM	0,036	4,25	-8,504
$Al_{88}Ni_{10}V_2$	IM	0,034	4,08	-90,144
$Al_{88}Ni_{10}Ti_2$	AM+IM	0,032	4,06	-10,136
$Al_{88}Ni_{10}Y_2$	AM+IM	0,05	5,55	-1,06,672
$Al_{88}Ni_{10}U_2$	*AM*	*0,03*	*4,29*	*-10,088*
$Al_{89}Mg_3Mm_8$	*AM*	*0,084*	*7,35*	*-2,572*
$Al_{87}Mg_5Mm_8$	*AM +IM*	*0,0869*	*7,43*	*-29,048*
$Al_{87}Mg_7Mm_6$	*AM+IM*	*0,0702*	*6,76*	*-25,872*
$Al_{85}Nb_6Ni_9$	*AM*	*0,0151*	*0,04*	*-11,052*
$Al_{85}Ta_6Ni_9$	*AM*	*0,0151*	*0,04*	*-11,234*
Multicomponent Al-LTM				
$Al_{88}Co_4Ni_4Cu_4$	IM	0,03	4,02	-5,85
$Al_{85}Co_5Ni_5Cu_5$	IM	0,05	4,43	-7,04
$Al_{85}Cr_3Mn_3Fe_3Co_3Ni_3$	IM	0,05	4,3	-8,42
$Al_{85}Cr_{2.5}Mn_{2.5}Fe_{2.5}Co_{2.5}Ni_{2.5}Cu_{2.5}$	IM	0,048	4,2	-6,94
Quaternaries with RE				
Al90Ni8Ce1Fe1	AM+IM	0,02	4,7	-8,19
Al85Ce5Ni8Co2	AM	0,017	7,35	-4,236
Al85Y5Ni8Co2	AM	0,016	7,1	-14,32
Al85U5Ni8Co2	*AM*	*0,049*	*4,5*	*-12,932*
Al85Ce8Ni5Co2	AM	0,058	8,22	-15,90
Composition	**XRD**	**λ**	**δ**	**ΔH (kJ/mol)**
Al85Y8Ni5Co2	AM	0,056	7,9	-16,005
Al85U8Ni5Co2	*AM*	*0,048*	*4.3*	*-1,38,032*
Al88Y7Fe5	AM	0.085	7,15	-1,13,132
Al88Y7Fe4Sb1	*AM*	*0,073*	*7,08*	*-1,10,272*
Al-Si based				
Al79Si10Ni9Ti2	*AM*	*0,09*	*7.85*	*-16,377*

The ΔH versus λ diagram is shown in Fig.2.a and 2.b. The atomic mismatch is calculated as a mean square deviation, δ, as well, in order to compare the Al-based alloys with the literature data published on various other metallic glasses (see Fig 3.a and Fig. 3.b).

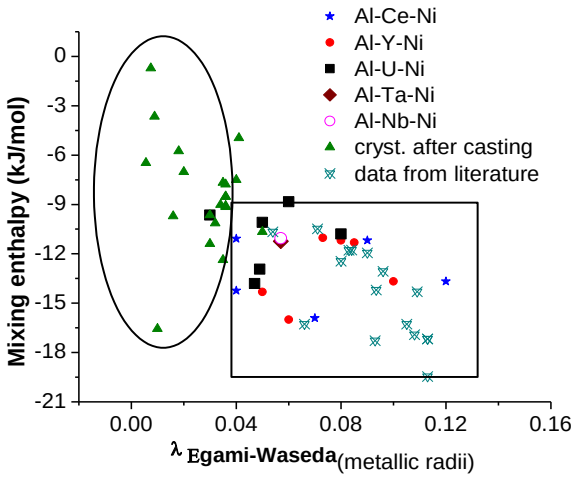

a)

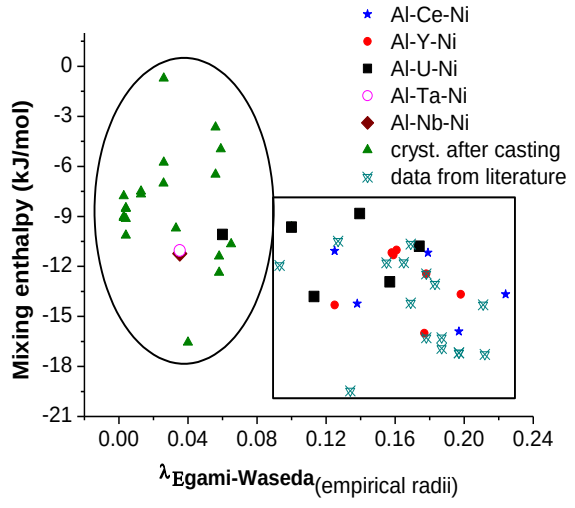

b)

Figure 2.a-2.b. Mixing enthalpy versus atomic mismatch expressed by Egami-Waseda parameter.

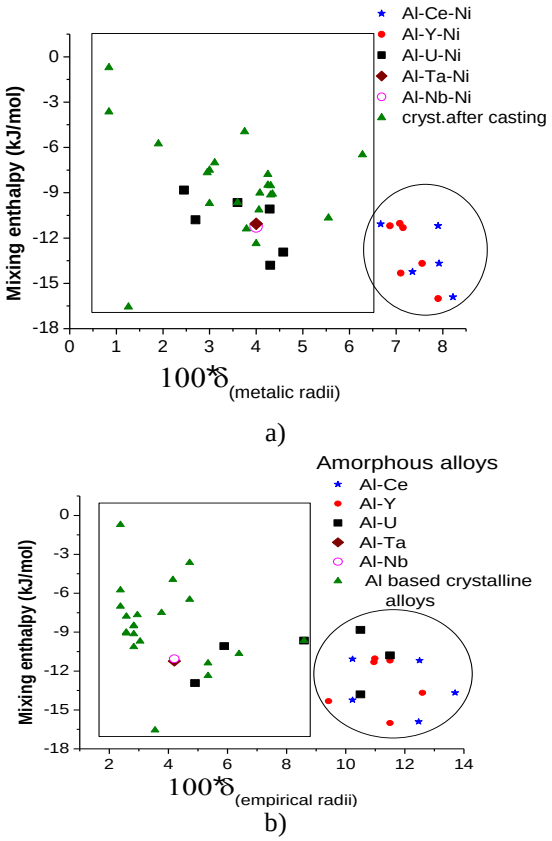

Figure 3.a-3.b. Mixing enthalpy versus atomic mismatch (expressed by mean square deviation of atomic radii, δ).

Perusal of Fig. 2. and 3. shows that the best separation of the amorphous and crystalline regions can be obtained using the Egami–Waseda parameter (deviation of atomic volumes), λ, based on metallic radii. Using the metallic radii however the λ parameter is smaller than the theoretically expected 0.1 value. Using the metallic radii the λ parameter becomes smaller than 0.1 and the overlapping of the amorphous and crystalline compositions is smaller and specially the novel amorphous compositions of this thesis lye in the crystalline region instead in the amorphous one.

Concerning the δ parameter for the atomic mismatch, which represent the deviation of metallic radii, the overlap between the crystalline and amorphous compositions is even more accentuated, especially for the new compositions.

Comparing these representations in Fig. 2 and 3, it turns out that the λ parameter gives the best separation between the amorphous and crystalline compositions. The range of variation for this δ parameter is rather limited for Al-based alloys comparing with the collected data for bulk amorphous alloy data [7].

The thermal stability and the mechanical strength are both determined by the bond strength which in metallic alloys are strongly dependent on the electron per atom, e/a, number in the given alloy. This is why a correlation is expected between the microhardness and crystallization temperatures for Al-based amorphous alloys covering wide composition range. In this way the GFA can be measured by the value of the microhardness as well. In the following we combine our data with the literature data and the observed correlation will be used for designing new high temperature Al-based amorphous alloys.

In the case of Al-based amorphous alloys, apparently little attention have been paid to the importance of the electronic structure governed by the average valence electron number per atom, z. Nagel and Tauc [8] studying the Pd-based metallic glasses, advanced the idea that the maximal stability of an amorphous structure is connected to the number of the valence electrons through the condition $2k_F = q_p$, where k_F is the wave vector at the Fermi level and $q_p = 4\pi\sin\theta/\lambda$, the location of the first peak in the structure factor. k_F can be calculated in the free electron approximation model as $k_F = (3\pi^2 n)^{1/3}$, where the free electron density, n, can be calculated as $n = zdN_A/<A>$, where d is the density, <A> is the average atomic weight and N_A is the Avogadro number.

The average valence electron number can be varied through the composition and in this way the condition for glass forming ability can be met.

The mechanical properties (such as, hardness and yield stress) are expected to show also a monoton variation with the number of outer electrons, e/a, as a consequence of the single phase nature of amorphous state. This relationship was demonstrated first for the transition metal–metalloid type glasses [9]. A similar systematic collection of the data as a function of outer electron number per atom is missing yet in the literature for the Al-based alloys.

We discuss the results of a systematic investigation of the effect of a wide range of alloying additions from periods 3, 4, 5 and 6 on the thermal – stability, hardness of Al-based metallic glasses containing RE elements. In addition, we discuss the effect of various RE elements and their concentration on the formation and stability of Al-based alloys.

There are many definitions of the valence electrons in the case of metals, especially in the case of transition metals. One of them considers all the outer electrons including the s, p, d and f electrons. e/a is the average outer (f + d + s) electron number:

$$e/a = 3\cdot X_{Al} + (3d+4s)\cdot X_{TM} + (f+d+s)\cdot X_{RE}$$

Another possibility is to take into account the definition of Pauling for the valence electrons as they are bonded in the crystalline state as it was used by the group of Inoue [10-11] establishing an electronic rule for the formation of glassy alloys (T_g versus VEC, valence electron concentration).

Finally the third possibility is to use the „bonding valence“to describe how many electrons does a given atom contribute to the Fermi sea. The bonding valence Z_B is defined with the help of the average electron density, n, at the boundary of the real–space Wigner–Seitz cell that surrounds each atom as $Z_B = n\Omega$, where Ω is the volume per atom in the elemental metal. Rose and Shore [12] estimated these densities from first principle muffin–tin density functional calculations. These three types of valences of the metals for the Al-based alloys are tabulated in Table 3.

Table. 3.

Element	e/a	VEC	Z_B
Al	3	3	2.76
Zn	2	-	2.4
Cu	11	5.8	2.57
Ni	10	6.2	2.83
Co	9	6.1	3.09
Fe	8	6.1	3.32
Mn	7	6	3.41
Cr	6	6	3.53
V	5	5	3.45

Ti	4	4	3.2
Sc	3	3	2.85
Ca	2	-	2.22
Mg	2	2.1	2.08
Y	3	3	3.21
Zr	4	4.5	3.75
Nb	5	5.4	4.14
Mo	6	6.1	4.42
La	3	3	3.5
Hf	18	4.6	3.97
Ta	19	5.5	4.51
W	20	6.3	4.79

Before collecting and comparing hardness data we have to perform some maximal load–to–hardness measurements on Al-based glassy alloys having different thickness in the range 10-40 μm. Micro-hardness of such thin ribbons can be measured on the surface of the ribbon or in the cross section after mounting in epoxy, grinding and polishing. The P_{max} versus HV relations have to be determined for both cases. As a rule for hardness measurements, the diameter of the indentation should be less then 7/10 of thickness, D< (7/10) t, for surface measurements and D< (1/5) t for indentations applied in the cross section. Based on the above correlations we adopt P_{max} = 20 g (or 10 g) for all the $HV_{0.01\text{-}0,02}$ measurements. The RE, U, and Ta containing amorphous ribbons were prepared for this work and the Zr and Fe, Co and Ni containing amorphous alloys have been collected from the paper of Inoue's group concerning the GFA of Al-Zr-LTM alloys [13-14].

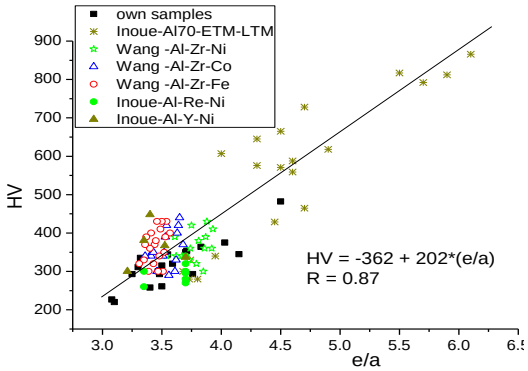

a)

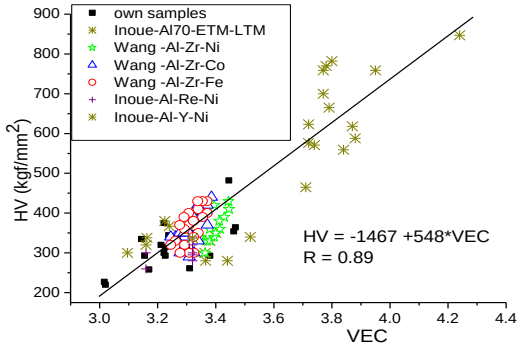

b)

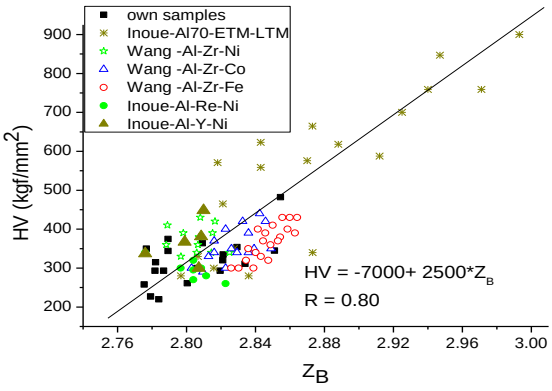

c)

Figure 4. Vickers hardness for Al-based amorphous alloys as a function of: a) total valence electron, e/a, b) Pauling valency, VEC,; c) bond valency, z_B The data are own collection from the literature in addition to our measurements on own compositions.

The best correlation has been obtained for the Pauling defined valence and for the total e/a electron numbers. Even more interesting is to join up these data obtained for Al-based alloys with the data obtained for other metallic glasses. In Fig. 5 a maximum can be observed around e/a = 6 ÷ 6.5 and VEC = 4.5, respectively, which denotes the highest strength and thermal stability. The scatter of the data can be understood taking into account the different sources of the data. Nevertheless, there is no doubt about the tendency towards a maximum.

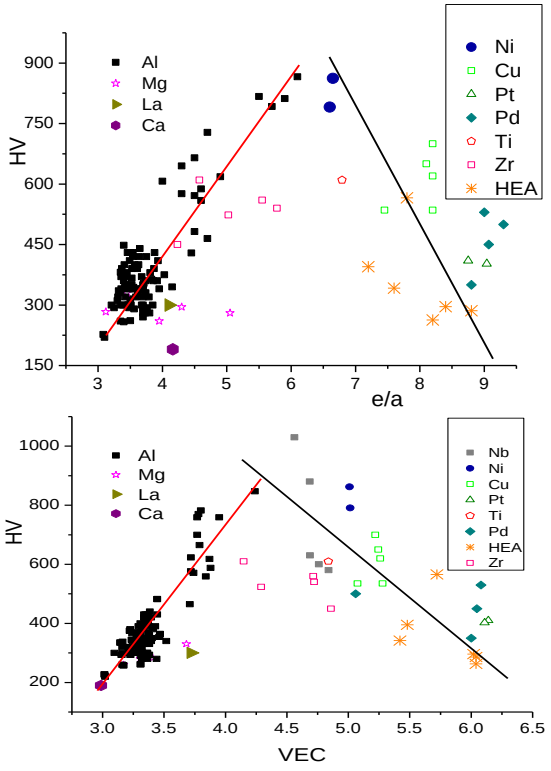

a)

Figure 5. Comparison of the hardness behavior of the amorphous alloys: a) as a function of total electron number, e/a, and b) as a function of Pauling valenc , VEC . The data are own collection from the literature concerning BMG's based on the indicated elements and some one-phase HEA alloys.

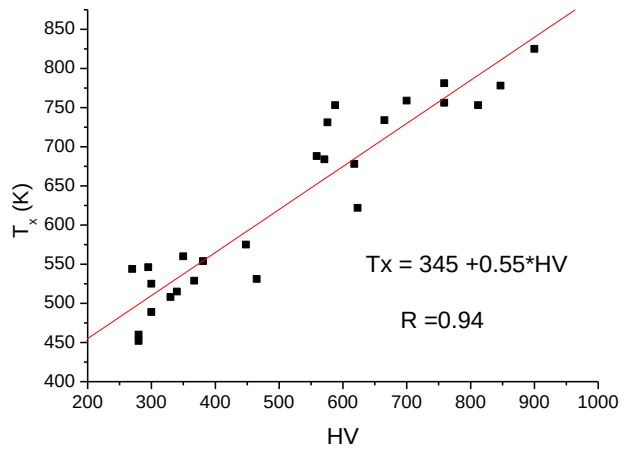

Figure 6. Correlation of crystallization temperature and hardness for Al–based amorphous alloys. The data are own collection from the literature in addition to our measurements on own compositions.

It is even more important the correlation we have found between the crystallization temperature and hardness values for the Al-base amorphous alloys. In Fig. 6 the collected data from the literature and our own data are represented. The correlation R = 0.94 is fairly good and denotes that the hardness can be taken as a measure for GFA of alloys with high temperature stability. Compositions with the largest e/a (or VEC) should be considered as a receipt for preparing Al-based amorphous alloys with high GFA.

In this paper we have presented an approach to estimate the GFA just using tabulated data of the elements only. This can be used for designing of amorphous alloys before any experimental action.

IV. Conclusion

We have applied data processing methods known in the literature for Al-based amorphous alloys (both for the own and literature data) which was useful to place the Al-based alloys among the other metallic glasses (based on Zr, Fe, Cu, etc.) based on some physical characteristics, like heat of mixing, atomic mismatch, crystallization temperature and hardness:

A combination of the heat of mixing (ΔH_{mix}) and atomic mismatch parameters has been used to assess the GFA of Al-based alloys. It can be stated that for Al-based amorphous compositions, ΔH_{mix} is between -9 and -20 kJ/mole whereas for bulk metallic glasses (based on Fe, Cu, Pd, etc.) ΔH is between -25 and -40 kJ/mole. The low GFA of Al- based alloys can be attributed to the relatively low heat of mixing and low relative atomic volume differences of the constituent elements. In addition, the lack of a deep eutectic at high Al-concentrations also contributes to the low GFA.

By analyzing the density data of Al-based amorphous alloys, I have demonstrated that the atomic volumes (i.e., the metallic radii) are conserved during alloy formation and the rule of mixture can be applied for the average molar volume.

A correlation was found between the crystallization temperatures and hardness values for the Al-based amorphous alloys. Furthermore, a correlation was found between the number of valence electrons and the hardness of Al-based amorphous alloys. In this way, an electronic rule for the formation of amorphous alloys with high thermal stability and strength could be established: the larger the average total electron number, e/a (or the Pauling valency, VEC), the better the strength and stability. Completing our results with the hardness data for other amorphous alloys from the literature, a maximum strength and thermal stability can be envisaged for the single-phase amorphous alloys for e/a around 6-6.5.

Acknowledgement

This work was supported by Hungarian OTKA 109570.

References

[1]. T. Egami, Y. Waseda, J. Non-Cryst Solids, 64, 1984, pp.134
[2]. S. Fang, X. Xiao, L. Xia, Q. Wang, W. Li, Y. D. Dong, Intermet. **12** (2004)1069
[3]. O.N. Senkov, D. B. Miracle, Mater. Res. Bul. **36** (2001) 2183
[4]. D.V. Louzguine-Luzgin and A. Inoue, J. of Non-Cryst. Solids **352** (2006) 3903
[5]. A. Takeuchi and A. Inoue, Mater. Trans. JIM **41** (2000)1372
[6]. J. Basu, B.S. Murty, S. Ranganathan, J. of Alloys and Comp. **465** (2008) 163
[7]. Y. Zhang, Y. J. Zhou, J. P. Lin, G. L. Chen, P. K. Liaw, Advanced Eng. Mater. **10** (2008) 534
[8]. S. R. Nagel and J. Tauc, Phys. Rev. Lett. **35** (1975) 380
[9]. L.W. Donald and H.A Davies, in: Proc. Conf. on Metallic Glasses, Science and Technology, Eds. C. Hargitai, I. Bakonyi and T. Kemény, **1** (1980)189
[10]. M. Fukuhara, M. Takahashi, Y. Kawazoe, and A. Inoue, Electronic rule for formation of glassy alloys, Appl. Phys. Letters **90**, (2007) 073114
[11]. M. Fukuhara, M. Takahashi, Y. Kawazoe, and A. Inoue, J. Alloys and Comp., 483 (2009) 623
[12]. J. H. Rose, H. B. Shore, Phys.Rev.B **43** (1991) 11605
[13]. L.Wang, L. Ma, H.Kimura, A. Inoue, Mater. Letters **52** (2002) 47
[14]. A. Inoue, Prog. in Mater. Sci. **43** (1998) 365
[15]. E. Fazakas and L.K. Varga , J. of Mater. Sci. and Tech., **15** (2007) 211
[16]. G. Wilde, H. Sieber and J. H. Perepezko**,** Scripta Mater. **40** (1999) 779
[17]. J.Q. Guo, K. Kita, K. Ohtera, J. Nagahora, A. Inoue, T. Masumoto, Mater. Letters **21** (1994) 279
[18]. A. Nordström, M. Ahlgren, Ö. Rapp, A. Inoue, Mater. Sci. and Eng. A **181** (1994) 921
[19]. L.Q. Xing**,** J**.** Eckert**,** W**.** Loser**,** and L**.** Schultz**,** Appl**.** Phys**.** Lett**. 74 (**1999**)** 664
[20].Laakmann, Mater. Sci. and Eng: A **173** (1993) 165
[21]. W.S. Sanders, J.S. Warner, D.B. Miracle, Intermetal. **14** (2006) 348
[22]. D.V. Louzguine, A. Inoue, J. of Non-Cryst. Solids **311** (2002) 281
[23]. V. Kwong, Y. C. Koo, S.J. Thorpe and K. T., Act. Met. Mat. **39** (1991) 1563
[24]. H.W. Yang, J. Wena, M.X. Quan, J.Q. Wang, J. of Non-Cryst. Solids **355** (2009) 235
[25]. C. Zhang, X. Bian, J. Guo, S. Wang, K. Song, C. Wang, B. Zhang, J. of Alloys and Comp. **436** (2007) 95
[26]. J.M. Dubois, K. Dehghan, P.Chieux and M. Laridjani, J. of Non-Cryst. Solids **93** (1987) 179
[27]. N. Bassim, C.S. Kiminami, M.J. Kaufman, J. of Non-Cryst. Solids **273** (2000) 271
[28]. R. D. S Lisboa, C.S. Kiminami, J. of Non-Cryst. Solids **304** (2002) 36